WORLD CONFERENCE ON TIMBER ENGINEERING 2025
BRISBANE, AUSTRALIA
Advancing Timber for the Future Built Environment

ADHESIVELY BONDED TIMBER-CONCRETE COMPOSITE BRIDGES – ANALYSIS OF THERMAL ACTIONS ON THE SUPERSTRUCTURE

Martin Kästner[1], Martin Ganß[2], Andreas Kirchner[3], Henri Paetow[4], Johannes Koch[5], Antje Simon[6], Matthias Kraus[7]

ABSTRACT: Timber-concrete composite (TCC) bridges are ecologically and economically appropriate alternatives to conventional, solid structures, especially in the span range of 10 to 30 m. The collaborative research Project 'HBVSens' aims to establish a new type of road bridge with continuous adhesive bonding between timber main girders and prefabricated concrete deck elements using a highly filled, tolerance-compensating polymer mortar. Based on initial investigations on a robust manufacturing technology and a suitable concept for quality assurance and structural health monitoring, an adhesively bonded timber concrete composite (ATCC) superstructure segment is set up for analysing the climatic impacts and evaluating the capability of different integrated sensors under environmental conditions. In this study, the manufacturing process of the hybrid superstructure element, the monitoring concept, and the sensor integration are elucidated. With a focus on the measured temperature changes and the corresponding structural reactions of the superstructure, first results of the investigations are presented.

KEYWORDS: timber-concrete composite, adhesive bond, bridge, temperature, monitoring

1 – INTRODUCTION

ATCC construction methods have been subject of repeated investigations since the 1960s in various design variants, including "wet-in-wet" bonding or bonding of prefabricated reinforced concrete components. In [1] an overview is given. To date, mainly the short-term load-bearing behaviour of ATCC components has been focused. In previous studies at the Bauhaus-University Weimar, mineral-filled polymer mortars based on epoxy resin (hereinafter also referred to as PC – polymer concrete) have proven to be suitable for the compensation of manufacturing tolerances between prefabricated components [1]. Due to large dimensions of TCC bridges the aspect of tolerance compensation is of major importance. Compared with the composite solutions used to date, which commonly rely on discontinuously arranged mechanical shear connectors (e.g. notches, stud connectors or bonded in connectors), the continuous adhesive bond between wood and concrete offers further mechanical and economic advantages. These include increased overall bending stiffness (wich allows a reduction in height of the superstructure) and load-bearing capacity as well as an improvement in quality due to the possibility of efficient prefabrication under controlled climatic conditions in the factory. Consequently, production and assembly times can be significantly reduced on the construction site - even compared to conventional solid construction methods.

Figure 1: Superstructure segment of an ATCC road bridge

Nevertheless, as bridge constructions aim for a service life of 100 years, the long-term load-bearing behaviour and durability of the bonding are of great importance. In this regard, the long-term hygro-thermal behaviour of ATCC components has been investigated in [2]. However, studies on the long-term behaviour of practically relevant bridge superstructures in an outdoor

[1] Martin Kästner, Bauhaus-University Weimar, Germany, martin.kaestner@uni-weimar.de
[2] Martin Ganß, Materials Research and Testing Institute at the Bauhaus-University Weimar, Germany, martin.ganss@mfpa.de
[3] Andreas Kirchner, Bauhaus-University Weimar, Germany andreas.kirchner@uni-weimar.de
[4] Henri Paetow, Bauhaus-University Weimar, Germany henri.paetow@uni-weimar.de
[5] Johannes Koch, University of applied Sciences Erfurt, Germany, johannes.koch@fh-erfurt.de
[6] Antje Simon, University of applied Sciences Erfurt, Germany, antje.simon@fh-erfurt.de
[7] Matthias Kraus, Bauhaus-University Weimar, Germany matthias.kraus@uni-weimar.de

https://doi.org/10.52202/080513-0094

climate have not been conducted yet. As the different thermal expansion coefficients of concrete and timber can lead to large constraining stresses, a major challenge regarding the structural design is to determine the thermal reactions within the hybrid structure precisely. Current design standards, such as DIN EN 1991-1-5 [3], only consider temperature profiles for superstructures made of steel and concrete. To analyse the hygro-thermal effects, temperature profiles, and the structural response under real climatic conditions, a segment of the superstructure of an ATCC road bridge has been set up and equipped with different sensors for quality assurance during manufacturing and for structural health monitoring (SHM) (Figure 1).

2 – MANUFACTURING PROCESS AND SENSOR SETUP

2.1 PRELIMINARY INVESTIGATIONS ON THE ADHESIVE JOINT CONFIGURATION AND THE BOND BEHAVIOUR

Based on inventigations on PC/wood composites at the TH Wismar between 1988 and 1993 [4] and subsequent further research work at the Bauhaus-University Weimar in cooperation with the Bennert GmbH [5] (e.g. regarding pull-off bond, shear and bending load-bearing behaviour) reinforcements of timber beams by adding a layer of PC in the compression zone have become state of the art for more than 10 years. Design and construction using the polymer mortar 'COMPONO 100 S' are covered by a national technical approval [6]. The PC consists of a cold-curing epoxy resin system (COMPONO) and a quartzitic aggregate mixture with a maximum grain size of 3 mm. In further research projects several PC-formulations with matched properties were investigated for diverse other adhesive bonding applications in timber engineering, e.g. in combination with steel, concrete, or composite materials based on carbon or glass fibres [7][8].

Comprehensive experimental studies on PC/concrete composites under shear-loading using the system 'COMPONO 100 S' have been presented in [1]. Three different pre-treatments of the concrete surface were tested within diverse test series: sandblasted, grinded and exposed aggregate surface (washed-out finish). Irrespective of the pre-treatment, the load capacity was limited by the shear strength of the concrete. However, a fracture surface lying particularly deep inside the concrete was only reached with exposed aggregate surfaces. As part of the ongoing research project "Hybrid timber bridges with adhesive bond - quality assurance and structural health monitoring using integrated sensors (HBVSens)", additional pull-off bond strength tests were carried out including variations in the pre-treatment of the concrete surfaces. The results confirmed that the surface should be profiled in order to prevent an adhesive failure at the PC/concrete interface. The better performance of an exposed aggregate surface compared to a sandblasted surface in terms of adhesion behaviour was also confirmed in delamination tests [9].

As for sandblasting, the process to produce exposed aggregate surfaces is an additional step in the prefabrication process of the precast concrete elements. Sandblasting requires special equipment and appropriate health and safety measures due to the dust exposure. However, exposed aggregate surfaces can be manufactured in any precast concrete factory with low equipment requirements and energy consumption. Therefore, the production of exposed aggregate concrete surfaces is preferred primarily for economic reasons. More detailed information on the pull-off bond strength test series and further composite shear tests is provided in [10].

The visco-elastic behaviour of the PC was studied using dynamic mechanical thermal analyses (DMTA) on small-sized PC prisms (10 x 10 x 60 mm). The specimens were testet under three-point bending (support distance 50 mm) using an High-Load-DMTA Eplexor 500 (Netzsch Gerätebau GmbH, Germany). The manufacturing, curing, and storage of the samples (for about four weeks after curing) up to testing were carried out at room temperature. The samples were tested strain-controlled in the linear visco-elastic regime with a dynamic loading frequency of 10 Hz and within a temperature range of -25 °C to 150 °C using a heating rate of 1 K/min. The average curves determined for two representative samples for the storage modulus E' and the loss factor tan δ are plotted in Figure 2. The onset of the dynamic glass transition as start of the 'softening' was determined from the E'-temperature-curve to approx. 53 °C (Tg,onset at 10 Hz). Above this temperature, a change in mechanical properties is to be expected – the material transitions into a softer, rubber-like state. Therefore, temperatures above Tg,onset should be avoided for ATCC structures.

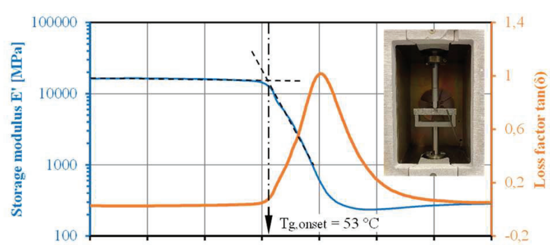

Figure 2: Storage modulus E' and loss factor tan(δ) as function of temperature of the PC from DMTA (frequency 10 Hz)

2.2 DESIGN AND CONSTRUCTION OF THE SUPERSTRUCTURE SEGMENT

The design of the superstructure segment is based on the results of a parameter study for TCC bridges [11]. The cross-section (Figure 4) represents half of a double-girdered T-beam cross-section required for a single-lane road bridge with a span of 10 meters. The segment

https://doi.org/10.52202/080513-0094

mainly consists of a block glued glulam beam (b x h = 100 x 60 cm, GL24h, spruce wood) and a prefabricated reinforced concrete slab element (b x h = 200 x 22 cm, C40/50). Using a surface deactivator (type HEBAU CSE pro 70), the concrete surface to be bonded was preproduced as an exposed aggregate surface with an expected washout depth of approx. 3 mm. As the thermal conduction in the grain direction of the wood is about twice as fast as in the transverse direction, the length of the superstructure segment was set to 2.5 meters, which corresponds to 2.5 times the width of the glulam beam. This allows a temperature analysis in the central part of the component over a length of approx. 50 cm, where the segment remains unaffected by the heat and moisture transport processes in the component's longitudinal direction.

Based on the results of the preliminary investigations summarized in chapter 2.1, 'COMPONO 100 S' was used as adhesive. However, sanding or planing the timber surface within 24 hours before bonding, as it is typically done, could not be undertaken due to the sensors that had already been installed. With respect to the maximum grain size of the aggregate mixture and the necessary tolerance compensation the thickness of the bond line was adjusted to approx. 10 mm. By means of appropriate formwork (Figure 3f) the adhesive mortar was applied in five stripes, each with a height of 18 mm.-Subsequently, the formwork was removed. The sufficiently stiff consistency of the fresh PC ensured that the stripe dimensions remained in a stable state until the concrete slab was placed (Figure 3g). The dead weight of the concrete slab was used to expand the stripes in width by compression to a final thickness of 10 mm. The objective was to achieve the best possible filling of the exposed aggregate structure on the concrete side and thus to ensure a close-fitting adhesive bond as free of voids as possible. To ensure optimal wetting and to improve adhesion at the PC/concrete interface, the exposed aggregate surface of the concrete slab was primed with the epoxy resin COMPONO just before placing the slab on the stripes (Figure 3e). In the design of the strip's geometry and spacing, care was taken to ensure that the amount of PC displaced by the concrete slab's dead weight was sufficient to grout the gaps between the strips, thus to achieve an almost full-surface bonding (Figure 3h). During bonding procedure no additional weighting or bonding pressure was needed.

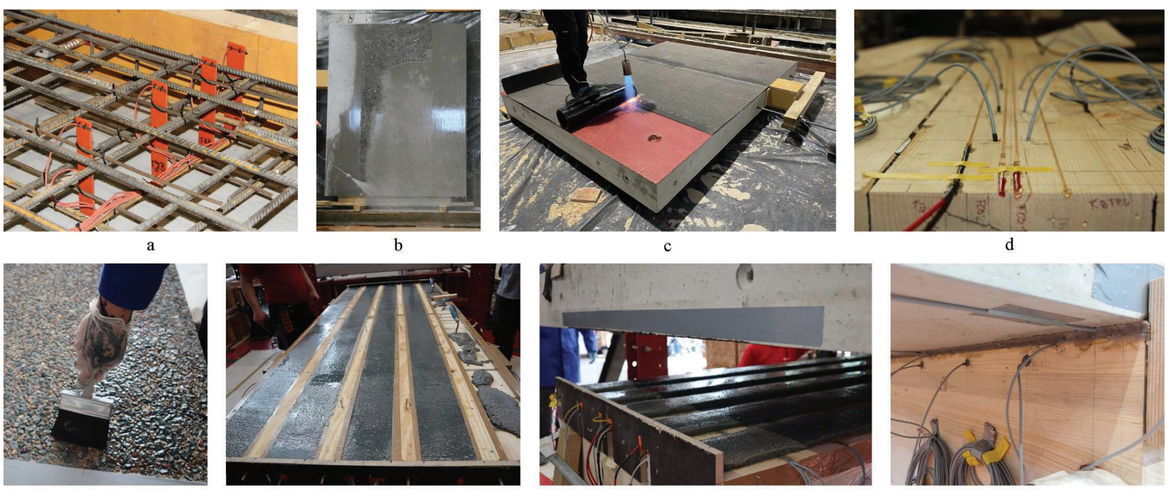
a b c d e f g h

Figure 3: Manufacturing process of the superstructure segment: a) Integration of PT elements in the concrete slab ;b) Manufacture of the exposed aggregate concrete surface; c) Application of the sealing system; d) Sensor integration on the bottom side of the block glued glulam beam; e) Priming of the exposed aggregates concrete surface; f) and g) Strip-shaped bonding; h) Completed adhesive joint

After the PC had hardened, the superstructure segment was transported to the site in the outdoor climate of Weimar. It was placed approx. 0.8 m above the ground to reduce the impact of the ground's temperature and moisture on the distribution of temperature and moisture of the superstructure segment. On site an 8 cm thick mastic asphalt layer was applied to the two-layer sealant that had already been bonded to the concrete slab in the factory (see Figure 3c and Figure 8). The mastic asphalt layer is required in order to record the effects of direct solar radiation on the temperature development in the superstructure realistically. Adequate weather protection of the timber is provided by the sealant and mastic asphalt on top of the concrete slab (as standardized for bridge decks in Germany [12]), the overhang of the concrete slab on both sides and by claddings at both end grain edges, see Figure 4. In addition, the south-facing end grain was vapour-tight sealed to prevent moisture diffusion between ambient air and this end grain.

2.3 SENSOR SETUP

The superstructure segment is used for the investigation of realistic moisture and temperature loads on the composite behaviour. This is implemented through permanent condition monitoring of temperature and timber moisture distributions in the component, as well as by monitoring strain changes in relevant component areas. For this purpose, different types of sensors were combined on the superstructure segment (see Figure 4 and Table 1). The sensor integration was carried out during and after the prefabrication of the components and was completed before bonding. A meteorological station is used to gather data on the outdoor environment.

The timber moisture is measured using the conventional electrical resistance method at a total of 32 measurement points inside the component, using stainless steel screws as electrodes. Further information on this subject as well as initial research findings are given in [13].

Temperatures within the component are primarily recorded using conventional thermocouples (PT 100 elements) based on the electrical resistance method as well. In the south-facing half of the component, a total of 72 PT elements were installed in five measurement planes (axes G, I, J, K, and L according to Figure 4): one for measuring the shade air temperature below the superstructure segment, twelve in the concrete slab, 45 in the glulam beam and 14 in the adhesive joint. Within the measurement planes the sensors are arranged at different heights at the center of the cross-section and, depending on the axis, with varying distances to the western edge of the component according to Figure 4. They were inserted into pre-drilled holes filled with thermal conductive paste at the corresponding positions in the wood, fixed on the wood top side and the bottom side of the concrete, or already attached to the reinforcement cage of the concrete slab before concreting (Figure 3a). The results of the temperature measurements inside the wooden component are also considered for temperature compensation of the timber moisture measurements. However, the timber moisture measuring points were mainly integrated in the north-facing half of the wooden component between axes A and G, to minimize mutual interference of the measurements, including from the measurement cables.

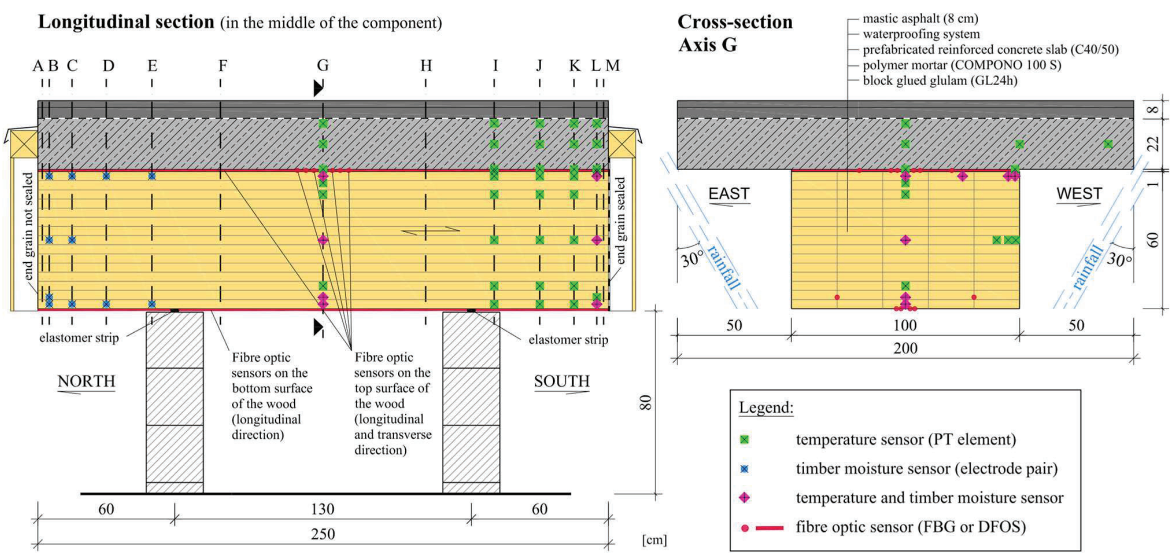

Figure 4: Superstructure segment: geometry, measuring planes and locations of the different sensors in the cross-section

Table 1: Sensor types and measurement methods

Sensor type	Measured variable	Measuring method
PT element	Temperature	Electrical resistance
Electrodes (stainless steel screws with insulated shaft)	Timber moisture content (TMC)	
Fibre Bragg Grating sensor (FBG)	Strains and temperatures (at discrete measuring points)	Reflected and/or transmitted light
Distributed fibre optic sensor (DFOS)	Strains (with high spatial resolution)	

Furthermore, different fiber optic sensors were applied on the top side as well as on the bottom side of the wood (Figure 3d). Both Fiber Bragg Grating (FBG) sensors and distributed fibre optic sensors (DFOS) were used. They enable either strain or temperature measurements, depending on the type of integration (rigidly fixed to the component or encapsulated in stainless steel capillaries). FBG sensors offer the possibility to record measurement values at predefined positions with high resolution and stability. The use of DFOS in combination with measurement of the rayleigh components in the backscatterd light by an optical frequency domain reflectometry (OFDR) allows the data acquisition with high spatial resolution over several meters of an optical fibre. The DFOS measuring technique offers great potential for comprehensive examination of timber and TCC structures as well as adhesive joints [14][15]. Detailed information and further insights in the results of the fiber-optical measurements are also given in [16].

Four FBG sensor fibers applied on the wood surface enable local strain and temperature measurement at a discrete measuring point in each of the 13 axes A to M. Additionally, five distributed measuring fibers were integrated along the length of the component, three on the

https://doi.org/10.52202/080513-0094

wood top surface, and two on the wood bottom surface. In the transverse direction of the component near axis G, three distributed measuring fibers were also integrated on the wood surface along with one encapsulated and one rigidly fixed FBG sensor fiber, each with six discrete measuring points.

3 – RESULTS

3.1 TEMPERATURE MEASUREMENTS

Following the start of monitoring in June 2023 (continuous measurement using PT elements and FBGs), additional measurement campaigns were carried out with the distributed fibre optic sensors.

Figure 5 shows the temperature developments for the year 2024 for the shade air temperature as well as for selected temperature measuring points inside the superstructure segment (according to Figure 6d). Due to its dimensions, the shading caused by the concrete slab, and heat storage capacity, the core of the wood reacts delayed to changes in the environment, while the concrete slab and the glued joint react more sensitively. In summer the temperatures in the concrete and the adhesive joint exceed the shade air temperature during the day due to solar radiation. The opposite is true at night. In winter, the components of the superstructure segment tend towards the shade air temperature, since the solar radiation is significantly lower than in summer. The marked times of the lowest shade air temperature, the maximum shade air temperature, and the maximum gradient in the component are particularly important for the strains on the superstructure segment.

Figure 6 displays the vertical temperature distributions in the component in section G for three relevant times. It shows the times of the minimum ($T_{air,min}$ = -13.9 °C; 10.01.2024 01:52 a.m.) and maximum ($T_{air,max}$ = 34.6 °C; 13.08.2024 04:14 p.m.) shade air temperature, which are discussed here as representative of a hot and cold period, as well as the time of the maximum temperature gradient (ΔT_{max} = 20.3 K; 09.07.2024 04:48 p.m.) in the superstructure segment.

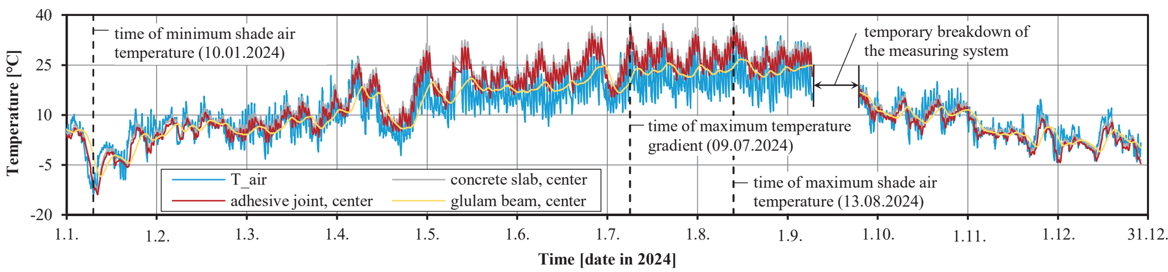

Figure 5: Results of the temperature measurements for the year 2024 for selected measurement points in cross-section G (locations see Figure 6d), and shade air temperature (blue line)

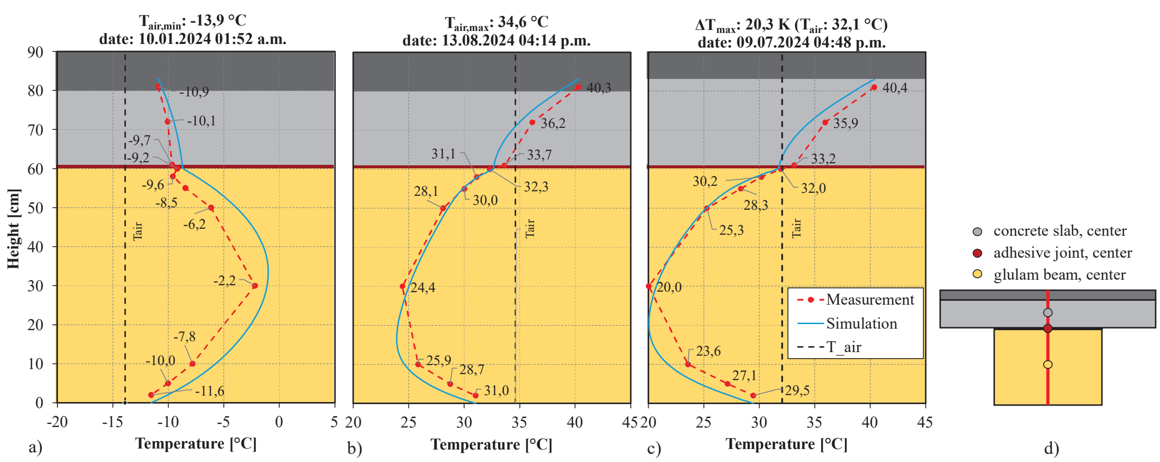

Figure 6: Vertical temperature distribution measured (red) and simulated (blue) in the cross-section G of the superstructure segment (along the red line in (d)) for the minimal external temperature (a), the maximal external temperature (b) and the largest temperature gradient (c).

With the 40.4 °C heated concrete slab and the approx. 20 °C warm core of the wood, the largest temperature gradient occures in the hot period. It can be assumed that the asphalt layer reaches even higher temperatures leading to increased gradients. In addition, the shading effect of the concrete slab on the timber component is clearly visible. Comparable temperatures are measured at the upper and lower edges of the timber component, with the core of the timber forming the coldest point of the component.

https://doi.org/10.52202/080513-0094

For the coldest day, it was observed that the temperature in the entire component fell below 0 °C. Lower temperature gradients occured than in summer. On the top and on the underside of the component, both temperatures tended towards the shade air temperature as a result of lower solar radiation in winter. The warmest point was in the core of the wood at approx. -2.2 °C, which is in line with expectations due to the heat-retaining properties of the wood (analogous to the coolest point in the hot period)

Irrespective of the hot and cold phases, an approx. linear temperature curve can be observed in the concrete slab, while the temperature in the timber component exhibits a highly non-linear and almost parabolic distribution.

Considering the results to date, it can be concluded that the most relevant temperature load case for a design results from the larger gradients of the hot period.

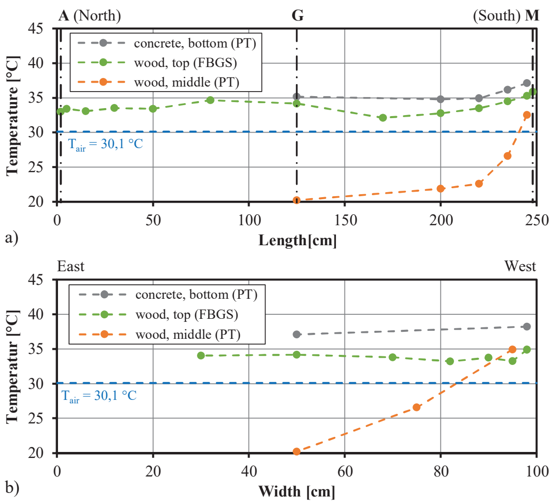

Figure 7: Temperature distributions at the height of the adhesive joint (grey and green dots/lines) and at the middle height of the block glued timber beam (orange dots/lines) at the maximum measured temperature in the adhesive joint (09.07.2024 06:47 p.m.); a) in longitudinal direction and b) in transverse direction of the superstructure segment

On July 9, 2024, the day of the largest climate-related temperature gradient in the component, also the highest adhesive joint temperature due to climatic temperature influences was recorded at 38.2 °C. For this time the temperature distributions at the height of the adhesive joint in longitudinal and transverse direction are shown in Figure 7. The maximum shade air temperature on that day was 32.2 °C and thus 6 K below the highest adhesive joint temperature and only 5 K below the maximum shade air temperature of 37 °C as assumed for Germany according to DIN EN 1991-1-5/NA [17]. Based on the measurement results obtained so far, it can be assumed that the climatic-related temperatures expected in the adhesive joint may have a sufficiently safety margin to the glass transition of the PC (Tg,onset = 53 °C, see chapter 2.1 and Figure 2). Softening of the adhesive joint and thus potentially associated changes in stiffness, strength, or bonding behaviour are therefore not expected as a result of ambient climate influences in Germany and countries with comparable summer climate conditions.

Figure 8: Paving of the approx. 230 °C hot mastic asphalt

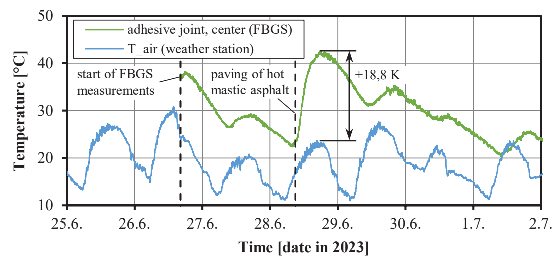

Figure 9: Development of the shade air temperature and the temperature in the adhesive joint of the superstructure segment during the period around mastic asphalt application

In addition to climate-related thermal influences, effects due to thermal actions arising during the mastic asphalt paving process should also be considered in the case of bridge assembly or maintenance. The application of the hot asphalt, which can reach temperatures of up to 230 °C, leads to a short-term, uneven heating of the superstructure. For the superstructure segment, the mastic asphalt layer with a thickness of 80 mm was applied at the test site (Figure 8). The paving process on June 28, 2023, was completed within one hour. Within approx. eight hours, a heating up of the adhesive joint to a maximum of 42.3 °C was registered (Figure 9). The maximum shade air temperature on that day was 23.6 °C and fluctuated between 11 °C and 31 °C (average 19.1 °C) within a period of about one week around June 28th. Despite these comparatively mild outside temperatures, the peak temperature achieved in the adhesive joint surpassed the maximum adhesive joint temperature resulting from climatic effects by approx. +4 K. To minimize the thermal stresses and internal constraints associated with the hot paving process, as well as in consideration of the previously mentioned safety margin to the glass transition temperature of the PC, it is advisable to avoid the installation of mastic asphalt on warm, sunny summer days with shade air temperatures well above 20 °C for ATCC bridges. Otherwise, hot paving should be appropriately considered as an additional thermal effect in the design and be superimposed with seasonal climate-related thermal effects (see prEN 1991-1-5 [18]).

https://doi.org/10.52202/080513-0094

3.2 STRAIN MEASUREMENTS

In addition to the temperatures, strain changes using fibre optic sensors are measured. As the glass fibres themselves are subject to changes in strain due to temperature, the measurement data must be temperature-compensated. This is done using encapsulated fibre optic sensors, which are not affected by mechanical, hygric, creep, and relaxation effects, as they are installed in a metallic capillary and only detect changes due to temperature. All measured strains are zeroed at the time of 01.07.2023 09:36 a.m.. Here, the temperature in the adhesive joint was approx. 20 °C, which corresponds to the temperature during the bonding process. Therefore, only strain changes will be evaluated subsequently.

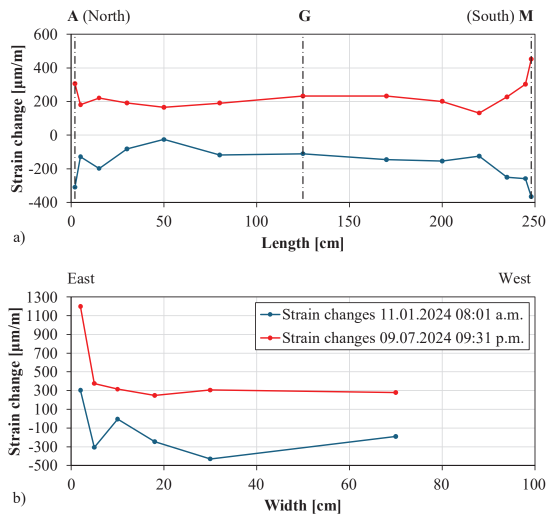

Figure 10: Distribution of measured strain changes with FBGS for the minimal and maximal measured strain changes in section G a) in longitudinal direction and b) in transverse direction

The greatest strain changes in section G were measured on 09.07.2024 at 09:31 p.m., i.e. the day with the largest temperature gradient in the component, and on 11.01. 2024 at 08:01 a.m., approx. one day after the minimum external temperature (see Figure 10). Shortly after the mastic asphalt was paved, similar strain changes were measured compared to the time of the largest temperature gradient. Over the period of almost half a year, in longitudinal direction this resulted in a strain difference regarding the adhesive bonded joint at section G of approx. 340 µm/m. The maximum strain difference of approx. 810 µm/m between the regarded points in time was measured at the edge of the component in section M. In transverse direction, the greatest strain difference was measured at the edge of the superstructure as well, with approx. 890 µm/m. As the edges of the component are subjected to greater thermal and hygric changes than the centre of the superstructure, this was to be expected. In addition, the influence of swelling and shrinkage is significantly greater transverse to the fibre than in the longitudinal direction.

3.3 INTERPRETATION AND NUMERICAL SIMULATION

The next steps focus on detailed analyses and comparisons with numerical simulation results to establish the basis for developing a temperature load approach for the design of ATCC bridges, which is currently not included in the relevant standards.

For this purpose, numerical models were created using ANSYS 2024 R1. In a transient temperature field analysis, hourly measured component temperatures were first applied and the resulting temperature field was then transferred to a transient mechanical structural analysis, allowing for the evaluation of strain states. Figure 11 depicts the procedure in the simulations considering the example of the cold period.

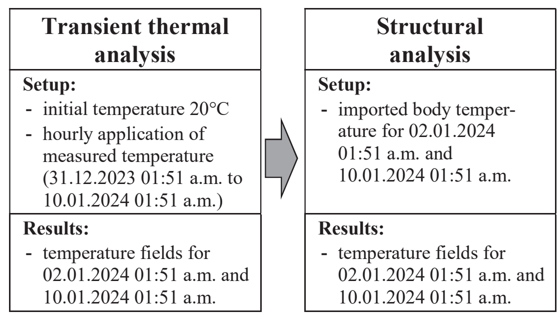

Figure 11: Procedure in the simulations as an exemplary case for the cold period

During a period of one week, the influence of moisture changes in the core of the superstructure is negligible, allowing for a better comparison of the simulation results with strain measurements in this time period. Moreover it takes around three days to obtain a reliable temperature field. Therefore, each simulation covers ten days before the actual point in time of interest (see Figure 11). The geometry was modelled as one-quarter of the superstructure segment utilizing symmetry conditions to consider the influence of the remaining real geometry. Subsequently, the temperatures measured at the component edge were applied. The contribution of solar radiation can thus be neglected, as it is already included in the measured temperature data. Table 2 shows the thermal material properties, which were calibrated such the temperature fields closely match the measured data.

Table 2: Thermal material properties used in the simulation

	Thermal expansion coefficient [10^{-6} 1/K]	Thermal conductivity [W/mK]	Specific heat capacity [J/kgK]
Concrete	13.0	2.5	1000
PC	25.0	2.3	800
Timber longitudinal	3.75	0.22	2100
Timber transversal	37.5	0.15	

In Figure 12 the geometry, mesh, and temperature field for the 09.07.2024 04:48 p.m. are shown. In Figure 6 a direct comparison of the measured and simulated temperature distributions over the superstructure height in section G for the three evaluated points in time is presented. The simulation results show good agreement with the measured temperatures, with deviations within the tolerance range of the sensors. The thermal material properties (Table 2) are therefore considered to be sufficiently validated. The coldest part of a component (the lower third in the timber) might not be captured by the measurement sensors, as no temperature sensor is installed in this area.

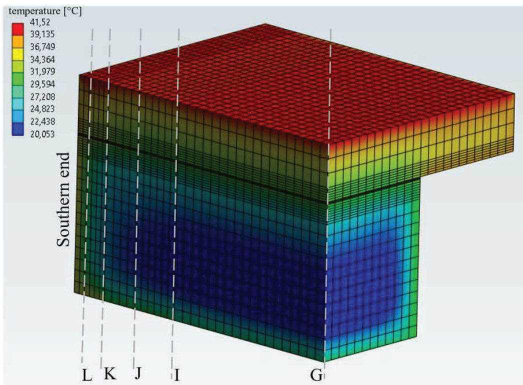

Figure 12: Geometry, mesh, and temperature field results of the simulation at the time of the maximum temperature gradient (09.07.2024 04:48 p.m.)

Subsequently, for strain comparisons, the focus is placed on the time point of the maximum temperature gradient ΔT_{max} within the component on Juli 9, 2024. Around that time, a large strain change was observed (see Figure 10). For better comparability and to minimize hygric and other time-dependent mechanical effects, the simulated and measured strains are related to a point in time exactly one week before the examined event and compared with each other. Here, the difference of total strains between the two points in time is determined. Figure 13a contrasts the strain changes from the simulation with the measured data in the adhesive joint along the longitudinal direction in relation to the starting point. In Figure 13b the changes in the strain distributions in transverse direction are compared with each other. The outside shade air temperature increased by 16.3 K between the two points in time of the period analyzed. Figure 13a shows that the trend of the simulated strain changes aligns well with the measured strain changes in longitudinal direction. The measured and simulated values mostly match in transverse direction (see Figure 13b).

Small deviations can be attributed to the aforementioned influencing factors, such as moisture changes, which are present in the measurement data but are initially not considered in the simulation, which only accounts for thermal influences. Particularly in the edge areas significantly higher strain changes are measured. These are presumably due to hygric expansion, among other factors. Furthermore, timber has a significantly higher swelling rate transverse to the fibre direction. This results in higher strain changes in transverse than in longitudinal direction. Additionally, the symmetry of the numerical modell does not take into account the effects of the ATCC's orientation with respect to the sky direction. In future a full numerical model can help to understand the impact of the orientation. Furthermore the influence of moisture as well as visco-elastic effects like creep and relaxation should be taken into account. Especially the influence of moisture is much stronger in the end grain area than in the centre of the superstructure segment.

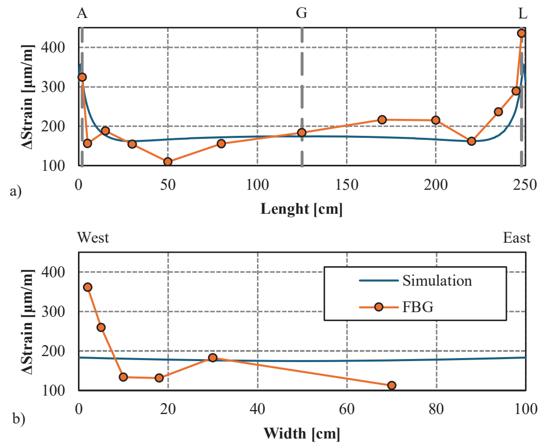

Figure 13: Horizontal strain changes measured and simulated in the adhesive joint at the selected time ΔT_{max} (09.07.2024 04:48 p.m.) a) in longitudinal direction and b) in transverse direction

For the cold period, the measured and the simulated changes in strain in longitudinal direction differ more than in summer. The reasons for this have not yet been conclusively clarified. The model, the measurement data, and the associated temperature compensation have to be investigated more in detail. In general, further research activities on the long-term load-bearing behaviour of ATCC components are required. While the behaviour of the superstructure segment under real outdoor conditions is being investigated over several years, further ongoing, accelerated experimental investigations within the research project aim to investigate the long-term effects of thermal influences on the short-term and fatigue load-bearing behaviour of adhesively bonded timber-concrete composite joint (see [10]).

4 – CONCLUSIONS AND OUTLOOK

Based on investigations regarding bond behaviour of adhesively bonded timber-concrete composites as well as design and manufacturing technology, an ATCC superstructure segment has been successfully set up. It is used to analyse the climatic impacts under environmental conditions and to evaluate the capability of different integrated sensors for quality assurance and SHM. To prevent adhesive failure at the PC/concrete interface, the concrete slab was prefabricated with an exposed aggregate surface in the bonding area. Regarding prefabrication and the joining process, this only required a small amount of additional work. Compensation for the textured concrete surface and the manufacturing tolerances was achieved by using a highly filled adhesive

https://doi.org/10.52202/080513-0094

system, which was applied in stripes to the timber surface. The strips were deformed and displaced in width and height when the slab was placed such an almost full-surface adhesive bond was achieved. Overall, the PC applied proved to be suitable for the production process – e.g. in terms of fresh mortar viscosity, processing time, and curing behaviour. The component demonstrator has been successfully installed outdoors and has been under monitoring for more than 1.5 years now.

In general, the superstructure segment itself has not yet shown any significant cracks that would indicate overstrain due to thermally-hygrometrically induced stresses. Potential structural damage cannot be recognised visually or with the strain measurements to date. The influence of moisture changes also turns out to be uncritical, as the load-bearing timber beam is well protected against weathering by the concrete slab. More information on moisture monitoring ist given in [13].

The analysis presented in this paper demonstrate that the sensor setup implemented on the superstructure segment is well suited to record temperature fields, as well as strains within a large ATCC component with high accuracy. Relevant for the decisive strain changes in the adhesively bonded joint are the time of the minimum outside temperature in winter and the time of the maximum temperature gradient in summer. Cold nights and subsequent summer days with high temperatures and high solar radiation are therefore more critical for the construction than periods with generally higher temperatures. As the fluctuation in daytime temperature is not as great in winter as in summer, it can be assumed that the lowest shade air temperatures cause the greatest strain changes in the component in winter.

In addition to climate-related thermal influences, effects due to the mastic asphalt paving were also analysed. Although the paving took place on a summer day with moderate shade air temperatures below 24 °C, the temperature within the adhesive joint reached a higher level compared with the summerday of the greatest climate-related temperature gradient. The paving of the mastic asphalt also caused similar strain changes compared to those measured at the time of the greatest temperature gradient. Therefore, mastic asphalt paving at shade air temperatures above 20 °C is not recommended and should otherwise be considered as a separate temperature load case. Overall, the temperatures measured in the adhesive joint so far have always been significantly below the glass transition temperature of the PC. So there is no risk of a softening of the joint due to climate-related heating of the superstructure.

A calibrated numerical model can map the effects of temperature changes on bonded ATCC bridges and calculate realistic temperature fields. The strain changes simulated with the model for short periods of time are in the same range as those measured. For most parts the strain curves agree with the locally measured strain values. However, influences from moisture changes, visco-elastic effects, and localised defects in the real component, have not yet been taken into account in the numerical model. Further research is needed to more accurately consider these influences and complex relationships in the material and numerical models.

5 – ACKNOWLEDGEMENT

Thanks go to the Fachagentur Nachwachsende Rohstoffe e.V. (FNR) and to the Federal Ministry of Food and Agriculture (BMEL) of Germany for funding the ongoing research project ‘HBVSens’ (FNR-project no.: 2221HV097). Special thanks go to partners from industry Bennert GmbH, STRAB Ingenieurholzbau Hermsdorf GmbH, Beton Fertigteilbau Erfurt GmbH, HEBAU GmbH, STRABAG AG, Sika Deutschland GmbH, FBGS GmbH, AOS GmbH and Polytec GmbH for strong support and fruitful discussion during the project. Thanks also go to the staff of the testing facility ‘Versuchstechnische Einrichtung’ at the Bauhaus-University Weimar and the MFPA for their support in the fabrication of the ATCC segment and for preparation and help during testing.

6 – REFERENCES

[1] M. Kästner: “Zum Tragverhalten von Polymermörtel-Klebverbindungen für die Anwendung bei Straßen-brücken in Holz-Beton-Verbundbauweise.” Bauhaus-Universität Weimar, Doctoral Thesis, 2019.

[2] L. Eisenhut: “Geklebter Verbund aus Holz und hochfestem Beton – Untersuchungen zum Langzeit-verhalten.” Universität Kassel, Doctoral Thesis, 2015.

[3] DIN EN 1991-1-5: “Eurocode 1: Einwirkungen auf Tragwerke – Teil 1-5: Allgemeine Einwirkungen – Temperatureinwirkungen.” 2010-12.

[4] K. Erler: “Verbundträger aus Holz und Polymer-beton.” research report, Technische Hochschule Wismer, Wismar, 1992.

[5] K. Rautenstrauch, K.-U. Schober, J. Frobel: “Innovative Verstärkung von Holztragwerken mit polymergebundenen Deckschichten im Verbund.” research report, Bauhaus-Universität Weimar, 2007.

[6] Deutsches Institut für Bautechnik: “Allgemeine bauaufsichtliche Zulassung Nr. Z-10.7-282: Polymer-verguss zur Verstärkung von Holzbauteilen.” Bennert GmbH Klettbach, 2021.

[7] M. Kästner, M. Jahreis, W. Hädicke, K. Rautenstrauch: “Development of continuous composite joints on the basis of polymer mortal with matched properties.” In: Proceedings of the World Conference on Timber Engineering (WCTE 2014), Quebec City, Canada, 2014.

[8] M. Kästner, W. Hädicke, M. Jahreis, K. Rautenstrauch: “High-Tech Timber Beam – a high-performance hybrid beam system made of composites

and timber.” In: Proceedings of the World Conference on Timber Engineering (WCTE 2014), Quebec City, Canada, 2014.

[9] J. Koch, A. Simon, P. Schumann: “Analysis of the durability of the adhesive joint of timber-concrete composite bridges.” In: Proceedings of the World Conference on Timber Engineering (WCTE 2025), Brisbane, Australia, 2025.

[10] A. Kirchner, M. Kästner, H. Paetow, M. Ganß, M. Kraus: “Investigations on adhesively bonded TCC-specimens under tensile, cyclic temperature and shear loading.” In: Proceedings of the World Conference on Timber Engineering (WCTE 2025), Brisbane, Australia, 2025.

[11] A. Simon: “Analyse zum Trag- und Verformungsverhalten von Straßenbrücken in Holz-Beton-Verbundbauweise.” Bauhaus-Universität Weimar, Doctoral Thesis, 2008.

[12] BASt - Bundesanstalt für Straßenwesen: “Zusätzliche technische Vertragsbedingungen und Richtlinien für Ingenieurbauten – ZTV-ING, Teil 6 – Bauwerksausstattung.” Bergisch Gladbach, 2022.

[13] J. Koch, A. Simon, M. Kästner, M. Ganß: “Analysis of the timber moisture content of an ATCC-road bridge superstructure segment.” In: Proceedings of the 5Th International Conference on Timber Bridges (ICTB 2025), Rotorua, New Zealand, 2025.

[14] J. Koch, M. Ganß, M. Kästner, A. Simon: “A promising approach of linear timber structural health monitoring.” In: Proceedings of the 13th World Conference on Timber Engineering (WCTE 2023), Oslo, Norway, 2023.

[15] M. Ganß, J. Hildebrand, H. Beinersdorf, M. Kuhne, C. Könke: “Monitoring von Klebverbindungen mittels faseroptischem Messsystem (MOFAS).” research report, DVS Forschungsvereinigung Band 304.

[16] M. Ganß, A. Kirchner, M. Kästner, J. Koch, A. Simon, M. Kraus: “Investigations on ATCC components using fiber-optical sensors for structural analyses.” In: Proceedings of the 5Th International Conference on Timber Bridges (ICTB 2025), Rotorua, New Zealand, 2025.

[17] DIN EN 1991-1-5/NA: “Nationaler Anhang – National festgelegte Parameter – Eurocode 1: Einwirkungen auf Tragwerke – Teil 1-5: Allgemeine Einwirkungen – Tempertaureinwirkungen.” 2010-12.

[18] prEN 1991-1-5: “Eurocode 1 – Actions on structures – Part-1-5: General actions – Thermal actions.” Draft, 2023-03.

 https://doi.org/10.52202/080513-0094